Mathematical Modelling and Analysis
Volume 11 Number 1, 2006, pages 73–86
 ISSN 1392-6292

ANALYSIS OF ANISOTROPIC VARIOGRAM MODELS FOR PREDICTION OF THE CURONIAN LAGOON DATA

I. KRŪMINIENĖ

Klaipėda University Faculty of Natural and Mathematical Sciences

H. Manto 84, Klaipėda, Lithuania

E-mail: ingrida@ik.ku.lt

Received May 17, 2005; revised February 3, 2006

Abstract. The anisotropy in particular environmental phenomena is detected when behavior of a physical process differs in different directions. In this paper geometric and zonal anisotropies are considered. Various methods of geostatistical analysis, also isotropic and geometrical anisotropic variogram models are compared and applied for the Curonian lagoon depth data. The results demonstrate that after robust estimation, i.e. elimination of outliers and after elimination of geometric anisotropy the precision of prediction and adequacy of models are much better. All computations have been performed by means of *gstat*, *base* and *spacial* packages of **R** system. Prediction results are compared with the results of research where outliers and geometric anisotropy were not eliminated.

Key words: variogram, robustness, trend, geometric anisotropy, zonal anisotropy, universal kriging

1. Introduction

For spatial locations $\{s_i = (x_i, y_i) : s_i \in D \subseteq R^2\}$, suppose we observe responses $Z(s_i), i = 1, ..., k$ where $\mathbf{Z} = (Z(s_1), Z(s_2), ..., Z(s_k))'$ are viewed as a vector of random field observations. The process Z is said to be *Gaussian* if, for any k $\geq$ 1 and locations $s_1, s_2, ..., s_k$, the vector $\mathbf{Z}$ has a multivariate normal distribution. The process Z is said to be *strictly stationary* if the joint distribution of $(Z(s_1), Z(s_2), ..., Z(s_k))$ is the same as that of $(Z(s_1 + h), Z(s_2 + h), ..., Z(s_k + h))$ for any k, spatial points $s_1, s_2, ..., s_k$, and any $h \in R^d$, provided only that all of $s_1, s_2, ..., s_k, s_1 + h, s_2 + h, ..., s_k + h$ lie within the domain D.

The process Z is said to be *second-order stationary* (also called *weakly stationary*) if $\mu(s) \equiv \mu$ (i.e., the mean is the same for all s) and

$$Cov(Z(s_i), Z(s_j)) = C(s_i - s_j), \quad \text{for all} \quad s_i, s_j \in D,$$

where $C(s)$ is the covariance function of observations at locations shifted by s. A *Gaussian* process which is second-order stationary is also strictly stationary (see [9], 35 p.).

Intrinsic stationarity is a weaker property than second-order stationarity. The variogram of intrinsic random function is written as

$$2\gamma(h) = Var\big[\big(Z(s_i) - Z(s_j)\big)\big].$$

The function $2\gamma(\cdot)$ is called the *variogram* and $\gamma(\cdot)$ the *semivariogram*. If the semivariogram (covariance) depends only on distance between locations the process is called *isotropic*.

Most of the geostatistical techniques are applied to a stationary data field. But in modeling the correlation structure of a spatial process $Z(s)$, the assumption of isotropy is often untenable. The spatial process $Z(s)$ is said to exhibit *anisotropy* when $C(s_i - s_j)$ depends upon both the magnitude and orientation of separation vector $(s_i - s_j)$. In literature there is some disagreement about the terminology used for describing the different kinds of anisotropy. Traditionally the term geometric anisotropy is used when the range changes with direction, while the sill is constant. This is the kind of anisotropy mostly observed in nature. Journel and Hiujbregts (1978) use the term zonal anisotropy for all kinds of anisotropy that are not geometric, e.g. the sill or both sill and range change with direction. According to Zimmerman (1993), anisotropy can take three forms: sill anisotropy, nugget anisotropy and/or range anisotropy. Isaaks and Srivastava (1989) use geometric anisotropy to describe changes of range with direction and constant sill, and zonal anisotropy when the sill changes while the range remains constant (see [4, 8] p. 45). In this paper the last definitions of *geometric and zonal anisotropy* will be used.

In our previous paper [7] the precision of the results obtained by two methods, i.e. kriging and cokriging, were compared by using cross-validation method. The results have showed that precision of predicted values is better when the cokriging method is used. Paper [5] presents maps of the predicted values in the whole Curonian lagoon, where the prediction is based on measurement data that are mentioned above. The general parameters of a semivariogram, i.e. sill, nugget and range are also described in this publication.

Further information about geostatistical analysis could be found in the books by N.C. Cressie [2] and J.P. Chiles and P. Delfiner [1]. Various types of variogram interpretation and methods of modeling could be found in [6].

In the previous research the process under studying was presumed to be isotropic. The objective of this research is the analysis of variograms in order to detect and eliminate geometric or zonal anisotropy. The data used in the study consist of depth measurements in 263 locations over a Curonian lagoon. The definition of two main anisotropy types and elimination of geometric anisotropy are introduced in Section 2 and also the universal kriging is described here. The results of the study are presented in Section 3.

2. Anisotropic Variogram Models

2.1. Estimation and modeling of the isotropic semivariogram

Determination of spatial variability is often based on a semivariogram. For isotropic random fields the sample estimator of the *classical semivariogram (variogram)* (Matheron, 1962), which is based on the *Method-of-Moments* (MoM), is defined as:

$$\hat{\gamma}(|h|) = \frac{1}{2N(|h|)} \sum_{(s_i,s_j)\in N(|h|)} [Z(s_i) - Z(s_j)]^2,$$

where $N(|h|)$ denotes all pairs (s_i, s_j) for which $|s_i - s_j| = |h|$ ([8], 38 p.). The classical variogram estimator is not robust against outliers in data. This may result in incorrect variances when estimating the value of the data by kriging. One of robust geostatistical procedures for data with outliers is the *variogram of order* $1/2$:

$$\hat{\gamma}(|h|) = \frac{1}{2N(|h|)} \sum_{(s_i,s_j)\in N(|h|)} \big[Z(s_i) - Z(s_j)\big]^{1/2} \Big/ \Big(0.457 + \frac{0.494}{N(|h|)}\Big).$$

This type of variogram has been developed by Cressie and Hawkins ([1], p. 41-44). By estimating and plotting both kinds of semivariograms (variograms), the influence of outliers can be examined (see [2]).

Potential models are compared with the estimated semivariogram and the best fitted model is used in the kriging estimation. Several methods have been proposed for fitting semivariogram models. One relatively simple method that appears to perform well is the *weighted least squares* method.

Isotropic processes are convenient to deal with because there is a number of widely applied parametric forms for $\gamma(\cdot)$, such as *linear, spherical, exponential, Gaussian* and others. An often used semivariogram model is linear and spherical one with the nugget effect. A reason for this is an easy interpretation of the parameters.

Figure 1*a* shows representation of a general variogram. Each variogram model is described by three variogram parameters: sill, nugget and range [1, 2, 4, 6, 3]. The linear isotropic semivariogram model with sill is defined as (see Fig. 1*b*):

$$\gamma(|h|) = \begin{cases} 0, & \text{if} \quad |h| = 0, \\ C_0 + C_1 \dfrac{|h|}{a}, & \text{if} \quad 0 < |h| \le a, \\ C_0 + C_1, & \text{if} \quad |h| \ge a. \end{cases} \tag{2.1}$$

The spherical isotropic semivariogram model (Fig. 1*c*) is given by:

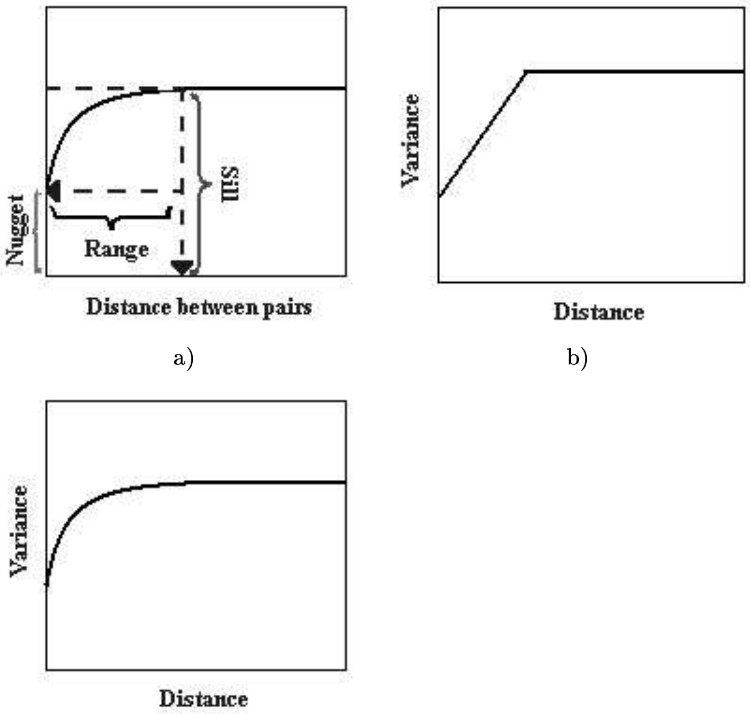

Figure 1. Representation of general variograms: a) idealized form of semivariogram function; b) linear semivariogram; c) spherical semivariogram.

$$\gamma(|h|) = \begin{cases} 0, & \text{if} \quad |h| = 0, \\ C_0 + C_1\Big[\dfrac{3}{2}\dfrac{|h|}{a} - \dfrac{1}{2}\Big(\dfrac{|h|}{a}\Big)^3\Big], & \text{if} \quad 0 < |h| \leq a, \\ C_0 + C_1, & \text{if} \quad |h| \geq a \end{cases} \tag{2.2}$$

where C_0 is the nugget effect, a is the range and $C_0 + C_1$ is the sill.

Traditionally fitting of the semivariogram is done by eye rather, because it has been shown that predictions computed by kriging are insensitive to the specification of the semivariogram model. The best semivariogram model can be found using the least squares criterion [8].

2.2. Directional detection and anisotropy variograms

Exploratory data analysis (EDA) techniques are often used to assess departure from isotropy: Kaluzny, Vega, Cardosa and Shelly (1996) propose directional semivariograms, Isaaks and Srivastava (1989) propose rose diagram and a contour plot of empirical semivariogram surface in R^2 (see [4]). In practice,

the directional semivariograms are often used. Semivariograms which utilize indiscriminately-oriented data pairs are called *omnidirectional. The directional semivariograms* are calculated using data location pairs of certain orientation, typically in four directions: N-S, E-W, NE-SW and NW-SE ($0^o, 45^o, 90^o$ and 135^o) for each lag with the tolerance angle 22.5^0 (see Fig. 2).

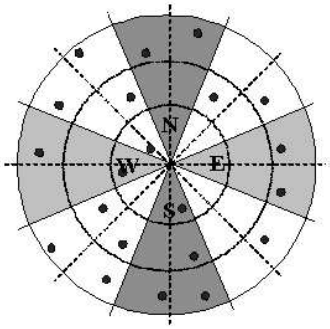

Figure 2. Direction, angle and tolerance of the directional semivariograms.

An anisotropy is said to be "geometric" when the directional semivariograms have the same shape and sill but different range values (Figure 3*a*). This is a situation in which Euclidean space is not suitable for measuring distance, but there may be a linear transformation of Euclidean space.

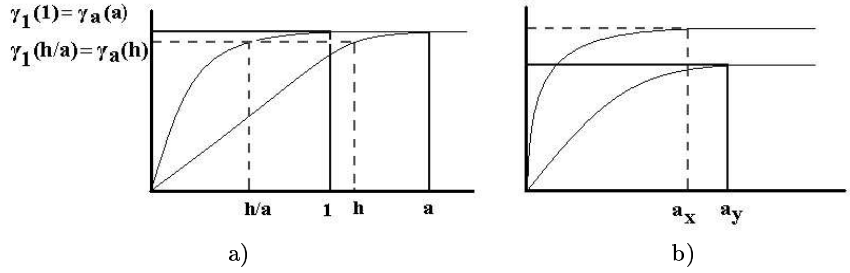

Figure 3. a) Geometric anisotropy; b) zonal anisotropy.

When the directional variograms show different variability in the different directions the sills are not comparable. In such case geostatistics can be used to establish a variogram model made up of components having a so-called "zonal" anisotropy (Fig. 3*b*). Pure zonal anisotropy is usually not seen in practice: typically it is occurs in combination with geometric anisotropy.

2.3. Elimination of geometric anisotropy

The basic procedure of correction of the geometric anisotropy is as follows:

- Identification of the directions for the maximum and minimum range.
- Rotation of the data axes to match directions of anisotropy.
- Reducing of the directional variograms to a single variogram with standardized range 1.
- Producing a single matrix **A** by multiplying matrixes of the rotation and distance scaling transformations.

The simplest case is when the anisotropy direction coincides with a coordinate axes (then no rotation is necessary).

The direction of maximum anisotropy rarely fall on one of the usual coordinate axes. We would like to express the distance h in terms of the anisotropic coordinate system rather than the usual coordinate system. Suppose that axes of anisotropy have been identified in direction (x', y') that differ from the coordinate system (x, y) by an angle of clockwise rotation α (2D case). If the directions of maximum and minimum range are orthogonal we can rotate the axes without changing any distance:

$$\begin{pmatrix} x' \\ y' \end{pmatrix} = \begin{bmatrix} \cos\alpha & \sin\alpha \\ -\sin\alpha & \cos\alpha \end{bmatrix} \begin{pmatrix} x \\ y \end{pmatrix}.$$

The variables in the rotated coordinate system are:

$$x' = x\cos\alpha + y\sin\alpha, \quad y' = y\cos\alpha - x\sin\alpha.$$

A vector $\mathbf{h} = (h_x, h_y)$ from the standard coordinate system can be expressed in the new coordinate system by transformation matrix **R**:

$$\mathbf{h}' = \begin{bmatrix} h'_x \\ h'_y \end{bmatrix} = \begin{bmatrix} \cos\alpha & \sin\alpha \\ -\sin\alpha & \cos\alpha \end{bmatrix} \begin{bmatrix} h_x \\ h_y \end{bmatrix} = \mathbf{R}\,h.$$

If the directions of maximum and minimum range are not orthogonal to each other then the transformed distance between s_i and s_j (where s_i and s_j are locations separated by a vector $\boldsymbol{h}$) $h = \sqrt{h'^2_x + h'^2_y}$, where h is the distance between locations s_i and s_j, $h_x = x_i - x_j$ and $h_y = y_i - y_j$. The distance transformation $\mathbf{h} \to \mathbf{h}'$ can be represented in matrix form

$$\mathbf{h}' = \mathbf{TRh} = \mathbf{Ah},$$

where

$$\mathbf{T} = \begin{pmatrix} \frac{1}{a_x} & 0 \\ 0 & \frac{1}{a_y} \end{pmatrix}, \quad \mathbf{A} = \begin{pmatrix} \frac{1}{a_x} & 0 \\ 0 & \frac{1}{a_y} \end{pmatrix} \begin{bmatrix} \cos\alpha & \sin\alpha \\ -\sin\alpha & \cos\alpha \end{bmatrix}.$$

Matrix **A** defines the transformation from the initial space, i.e. a circle of radius a (see Fig. 4*a*), to the isotropic space, i.e. an ellipse, which is a linear

transformation of a circle (see Fig. 4*b*). Here a_i is chosen positive number, α is often taken as the direction of maximum range and a_x/a_y is the *anisotropy ratio*, which is is the ratio of the minor range to the major range and its value is between 0 and 1 ([1], p. 94). The variogram can therefore be written as

$$\gamma(h) = \gamma_0(|\mathbf{Ah}|).$$

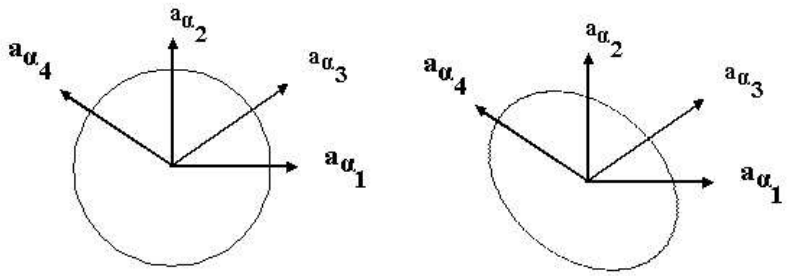

a) b)

Figure 4. a) Isotropy case (a circle of radius a), b) geometric anisotropy case (an ellipse).

2.4. Universal kriging

Kriging is a procedure for spatial prediction at an unobserved location, using data at observed locations, optimized with respect to a specific error criterion. Basic model for kriging is given by

$$Z(s) = \mu(s) + \delta(s), \quad s \in D, \mu \in R,$$

where μ denotes the unknown population mean function. This can also be regarded as the *trend, signal*, or *large-scale spatial variation.* The correlated error process is given by

$$\delta(\cdot) \equiv W(\cdot) + \eta(\cdot) + \varepsilon(\cdot),$$

here $W(\cdot)$, $\eta(\cdot)$, $\varepsilon(\cdot)$ are smooth small-scale variation, micro-scale variation, measurement error or noise, respectively (see [2], 113 p.)

Universal kriging assumes that mean value $\mu(s)$ of $Z(s)$ can be expressed as linear combination of known functions $f_1(s), ..., f_q(s)$:

$$\mu(s) = \beta' \mathbf{f}(s), \quad \mathbf{f}(s) = (f_1(s), ..., f_q(s))', \quad \beta \in R^q.$$

Thus

$$Z(s) = \sum_{l=1}^{q} \beta_l f_l(s) + \delta(s).$$

For instance, in our case where $Z(s)$ is a random process representing Curonian lagoon depth $\mu(s)$ is the third order trend surface:

$$\mu(s) = \beta_1 + \beta_2 x(s) + \beta_3 y(s) + \beta_4 x(s)^2 + \beta_5 x(s)y(s) + \beta_6 y^2(s) + \beta_7 x^3(s) + \beta_8 x^2(s)y(s) + \beta_9 x(s)y^2(s) + \beta_{10} y^3(s)$$

and $q = 10$. The value $Z(s_0)$ of the random process Z at location s_0 is given by

$$Z(s_0) = \beta' \mathbf{f}(s_0) + \delta(s_0).$$

According to the universal kriging theory, the linear predictor $\hat{Z}(s_0)$ of the value $Z(s_0)$ can be expressed as a linear combination of the measured values $Z(s_k)$ at n locations:

$$\hat{Z}(s_0) = \sum_{k=1}^{n} w_k Z(s_k),$$

where w_k is the weight for the observation $Z(s_k)$, which are chosen to minimize the mean squared error $MSE = E(\hat{Z}(s_0) - Z(s_0))^2$, $\hat{Z}(s_0)$ is unbiased for $Z(s_0)$ if $\sum_{k=1}^{n} w_k = 1$.

The variance of the universal kriging predictor:

$$\sigma^2_{ukrig} = \sum_{k=1}^{n} w_k \gamma(s_k - s_0) + m_0 + \sum_{l=1}^{q} m_l f_l(s_0),$$

where $m' = (m_0, ..., m_l)$ is a vector of Lagrange multipliers. The details can be found in [2].

3. Results and Discussions

3.1. The data

Procedures of robust estimation, directional semivariogram model fitting, and universal kriging were applied to the depth data of the Curonian lagoon. The Curonian lagoon is a large (length 95 km, width up to 48 km) shallow (mean depth of 3.8 m, the maximum 5.8 m) coastal water body in the south-eastern part of the Baltic Sea. The outlet of the lagoon to the Baltic Sea, Klaipėda Strait, is artificially deepened down to 12 m. The data have been collected in 1990 by S. Gulbinskas. It consists of bed sediments and depth data of the Curonian lagoon. In this research only depth data of the Curonian lagoon was used. The depth was measured at 263 locations. Their x coordinate values are between 278199 and 333376 and y coordinate values are between 6088178 and 6172784. The locations of the measurements of the Curonian lagoon depth data are shown in Figure 5*a*.

For data analysis and mapping *R* system packages *base, spatial* and *gstat* have been chosen. They are available for free on

`http://www.GSTAT.org/GSTAT.pdf`.

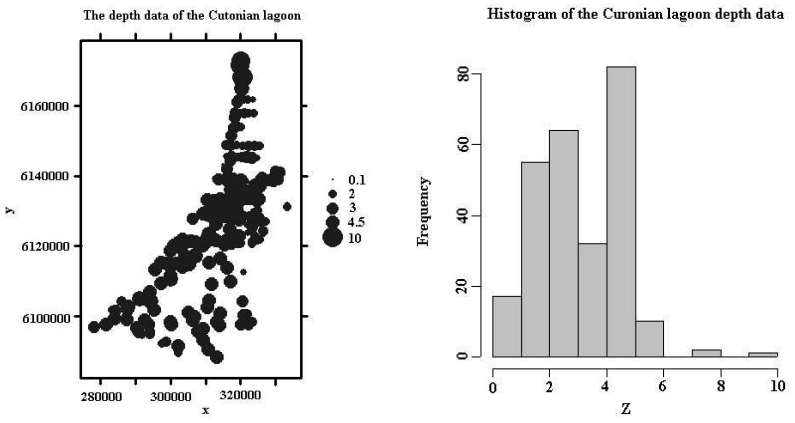

a) b)

Figure 5. a) Locations of the depth measurements, b) the histogram of the depth data.

There are the other packages in *R* for geostatistical analysis, e.g. *fields, geoR, geoRglm, gstat, spatial.*

Package *gstat* is a program for modelling, prediction and simulation of geostatistical data in one, two and three dimensions. The package provides prediction and estimation using a model that is the sum of a trend modeled as a linear function of polynomials of the coordinates or of user-defined base functions, and an independent or dependent, geostatistically modeled residual. This allows simple, ordinary and universal kriging, simple, ordinary and universal cokriging, standardised cokriging, kriging with external drift, block kriging and "kriging the trend", as well as uncorrelated, ordinary or weighted least squares regression prediction.

3.2. Data analysis by descriptive statistical methods

The histogram of the sampled depth data is given in Figure 5*b*. The depth data is positively skewed and may be this is a reason of extreme values of data.

The summary statistics of the depth data with outliers and without outliers are presented in Table 1.

Table 1. Summary statistics of depth data.

	Minimum	Maximum	Mean	Standard deviation
with outliers	0.100	10.000	3.161	1.5224
without outliers	0.100	8.000	3.135	1.4651

As described in Section 2.1, the estimation and plotting of the classical and robust semivariograms can be used to examine the influence of outliers. ANOVA analysis, partially presented in Table 2, shows that *Multiple* R^2 the trend is the largest for the third order polynomial. Thus we can conclude that the depth data constitute to the third order polynomial trend, which has the following drift coefficients:

$$\beta' = (2.9194,\ 3.3264,\ -3.8400,\ -2.3292,\ -6.8664,\ 8.1018,\ 0.5259,\ -3.2525,\ 5.1536,\ 4.0109).$$

Here L, Q, P denote linear, quadratic and polynomial trends, respectively.

Table 2. The partial results of the ANOVA tables.

Trend type:	Mult. R^2:	Fitted:					Residuals:				
		Min	1Q	Med.	3Q	Max	Min	1Q	Med.	3Q	Max
L	0.1094	2.440	2.776	2.983	3.401	4.660	-3.777	-0.919	0.042	1.055	5.286
Q	0.2109	1.188	2.713	3.164	3.738	4.117	-3.855	-0.844	0.207	0.906	5.266
P	0.3581	0.114	2.477	3.106	3.761	4.944	-3.999	-0.727	0.121	0.811	4.040

Figure 6*a* presents estimated model of classical omnidirectional semivariograms without third order polynomial trend and *b* part of the figure shows analogous graph for robust estimates of omnidirectional semivariograms for nontrended data without trend elimination. The estimates of extreme value, depth of 10 m, significantly influence the behaviour of variograms.

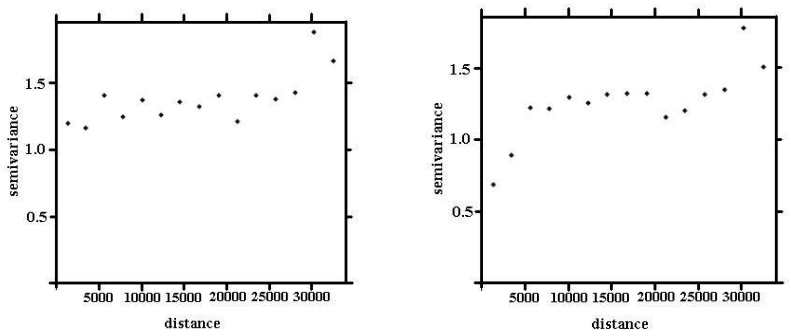

a) b)

Figure 6. a) Omnidirectional (classical) semivariogram for depth data without eliminated trend (with outliers), b) omnidirectional (robust) semivariogram of depth data (without eliminated trend and outliers).

The directional semivariograms are calculated in four directions N-S, E-W, NE-SW and NW-SE ($0^o, 45^o, 90^o$ and 135^o clockwise from north) for each lag with the tolerance angle 22.5^0 to identify the anisotropy directions and to find parameters for the optimal semivariogram model. The parameters of directional linear and spherical semivariogram models are presented in Table 3.

Table 3. Variogram parameters for directional variograms.

Direction	Linear model			Spherical model		
	Sill	Nugget	Range	Sill	Nugget	Range
0:	1.31	0.4843	4177.81	1.31	0.3741	5058.37
45:	1.15	0.3445	6978.73	1.18	0.3429	10372.08
90:	1.30	0.5809	7869.18	1.29	0.5519	9924.36
135:	1.37	0.5490	7368.99	1.39	0.5270	10207.5

The results demonstrate that the sill in four directions for all semivariogram models is almost the same, but the range is different. Thus, we can focus our attention on the case of geometric anisotropy. The highest range for the linear model is detected in the direction 90^0 clockwise from north, for spherical model in the direction of 45^0, while the smallest range for both models is found in the north direction. Consequently, the anisotropy ratio for the each semivariogram model is calculated and the semivariogram models estimated in these directions. The estimates of semivariogram models are given in Table 4.

Table 4. Anisotropy ratios and the minimized sum of the squared residuals.

Type of semivariogram model	Anisotropy ratio	The minimized sum of the squared residuals
Linear	0.531	0.00000796
Spherical	0.488	**0.00000788**

From Table 4 we deduce that the spherical semivariogram model is better. The fitted robust directional semivariogram for spherical model is presented in Figure 7. Now the best fitted semivariogram model can be used in the kriging prediction procedure. As described in Section 2.4, the universal kriging is used when the mean field can be described by a linear (with respect to parameters) trend model. The universal kriging models have been evaluated and compared for the depth data of the Curonian lagoon for the two different cases:

1) outliers and geometric anisotropy is eliminated,
2) outliers and geometric anisotropy is not eliminated.

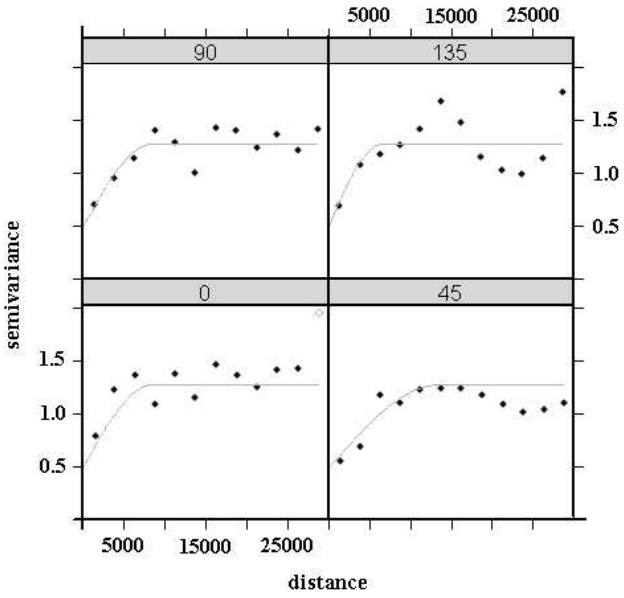

Figure 7. The fitted robust directional semivariogram for spherical model.

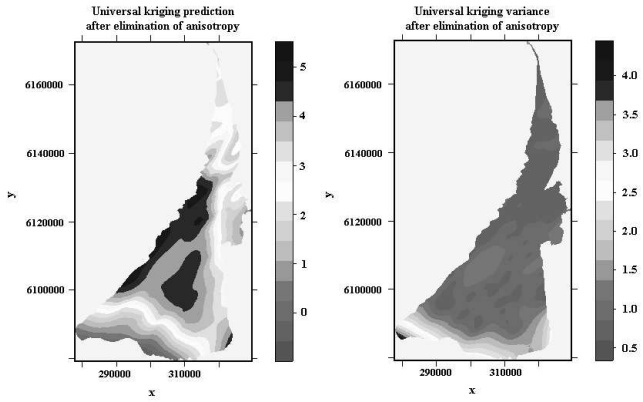

Figure 8. The universal kriging prediction and variance maps when outliers, trend and geometric anisotropy is eliminated.

Maps of the results are presented in Figure 8 and Figure 9. The summary statistics of these maps are given in Table 5.

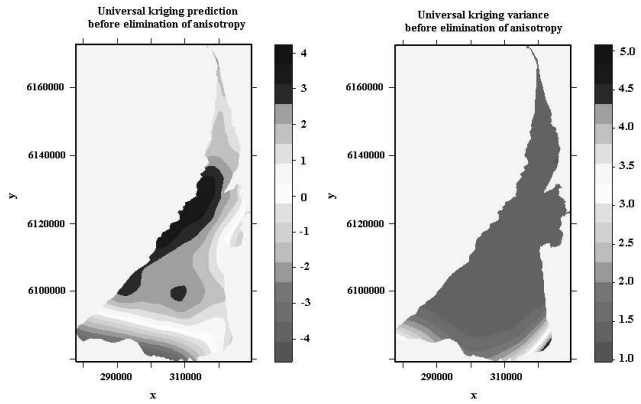

Figure 9. The universal kriging prediction and variance maps when outliers and geometric anisotropy is not eliminated.

Table 5. Summary statistics of prediction and variance maps of two universal kriging method.

	Values of prediction			Values of variance		
The case	Minimum	Maximum	Mean	Minimum	Maximum	Mean
1)	-4.0976	3.6851	1.2398	1.225	4.833	1.487
2)	-0.5956	5.1270	3.1038	0.5843	4.1987	1.1110

The summary statistics in Table 1 and Table 5 prove that the universal kriging prediction with eliminated outliers and geometric anisotropy is more realistic (more close to the true depth data).

4. Conclusions

The main focus of the study was geometric anisotropy, which is a special case of anisotropy, and occurs when the spatial dependence changes with direction in an elliptical fashion. The effects of geometric anisotropy on the prediction of the Curonian lagoon depth data was analysed.

Results demonstrate that:

1. The depth data have asymmetric distribution with a left tail by reason of one extreme value 10 meters depth.
2. The spatial process of the depth data constitute to the third order polynomial trend.
3. The sill of four directional semivariogram spherical and linear models is almost the same, when the range is different. This is case of geometric anisotropy.

4. Spherical model best describes semivariance of depth data.
5. Prediction results of the depth data after elimination of outliers and geometric anisotropy made by universal kriging shows that variation of data are more close to the mean value.

Detailed work is required to test anisotropy influence on cokriging estimation of depth data of the Curonian lagoon for mine planning purposes. Optimal methods of depth estimation will continue to be explored.

References

[1] J. P. Chiles and P. Delfiner. *Geostatistics: Modeling Spatial Uncertainty.* John Wiley, New York, 1999.
[2] N. Cressie. *Statistics for Spatial Data.* John Wiley, New York, 1993.
[3] K. Dučinskas and J. Šaltytė-Benth. *Erdvinė statistika.* Klaipėdos universiteto leidykla, 2003.
[4] M.D. Ecker and A.E. Gelfand. Bayesian modeling and inference for geometrically anisotropic spatial data. *Mathematical Geology*, **31**(1), 67 – 83, 1999.
[5] R. Garška and I. Krūminienė. Spatial analysis and prediction of Curonian lagoon data with gstat. *Mathematical Modelling and Analysis*, **9**(1), 39 – 50, 2004.
[6] E. Gringarten and V. Deutsch. Teacher's aide variogram interpretation and modeling. *Mathematical Geology*, **33**(4), 507 – 534, 2001.
[7] I. Krūminienė, K. Dučinskas and R. Garška. Applying of kriging and cokriging methods for prediction of Curonian lagoon data. *Liet. matem. rink.*, **43**, 504 – 508, 2003.
[8] Soren Nymand Lophaven. *Reconstruction of data from the aquatic environment.* Lyngby TU, 2001.
[9] R. Smith. *Environmental Statistics.* Department of Statistics, 2001.